Available online at www.sciencedirect.com
SCIENCE DIRECT®
Chemical Engineering and Processing 44 (2005) 1207–1215
Chemical Engineering and Processing
www.elsevier.com/locate/cep

Multi-fields synergy in the process of reactive distillation coupled with membrane separation

Huajun Wang, Bolun Yang *, Jiang Wu, Guosheng Zhao, Xianhu Tao

Department of Chemical Engineering, Xi'an Jiaotong University, Xi'an, Shaanxi, China

Received 28 April 2004; received in revised form 17 August 2004; accepted 11 March 2005
Available online 13 June 2005

Abstract

A new method for analyzing reactive distillation coupled with membrane separation system was proposed with the viewpoint of non-equilibrium thermodynamics and the phenomenological theory. The synthesis of ethyl *tert*-butyl ether was chosen as a model system. The synergy of multi-fields such as temperature, concentration and chemical potential in this combined process was discussed; the relationship of each vector within a field was investigated by considering both of Soret effect and Dufour effect. The equations of mass and heat fluxes were established and the coefficients for both of them were obtained with the condition of the synergy in multi-fields. It can be known from the research results that the mass and heat transfer rate were increased or decreased with the synergy of multi-fields; the direction of transfer was also changed by the effect of synergy of multi-fields. From the viewpoint of field synergy, the model of non-equilibrium stage for the reactive distillation coupled with membrane separation was developed. The model incorporated complex reaction kinetics, vapor–liquid non-idealities, distillation and pervaporation process. The rapid solution for this model can be obtained by Newton–Raphson method. Simulation results are in good agreements with the experimental results.

Keywords: Reactive distillation; Pervaporation; Heat and mass transfer; Non-equilibrium; Synergy

1. Introduction

Reactive distillation is a multifunction reactor concept combining chemical reaction and distillation. The integration of reaction and separation in one unit may yield several advantages such as better conversions, higher selectivity and reduced energy compared to conventional reactor-separation sequences. This technology has made significant progress in recent years, both in industrial application and in scientific research.

A reactive distillation process combined with pervaporation was proposed in our previous work [1,2]. In this new process, a membrane separator and a reactive distillation column formed the system. The reactive column was consists of three zones: such as rectification zone, stripping zone and reaction zone. It was assumed that the reaction occurred in the liquid phase on the reaction zone like general reactive distillation process. However, the residue in the reboiler was pumped into a membrane separator where most by-products were separated, and then, it was returned back to the reboiler. Thus, the efficiency of reactive distillation can be increased. The mechanism of the membrane separation was explained with the dissolution–diffusion model. A mathematical model for this system was also developed. However, the theory analysis for this kind of multi-unit operation process was still carried out based on the viewpoint of traditional chemical engineering. The interaction between mass transfer, heat transfer and the chemical reaction was not considered in our previous research.

In this work, the phenomenological theory was used to analyze the multi-fields synergy in the new combined process of reactive distillation with membrane separation. The interaction between mass transfer and heat transfer was investigated and the coefficients of mass and heat transfer were obtained based on the analyzing the multi-fields synergy. A

* Corresponding author. Tel.: +86 29 82668980; fax: +86 29 83237910.
E-mail address: blunyang@mail.xjtu.edu.cn (B. Yang).

0255-2701/$ – see front matter © 2005 Elsevier B.V. All rights reserved.
doi:10.1016/j.cep.2005.03.007

new model was developed to describe this combined process more correctly.

2. Non-equilibrium theories

2.1. Thermodynamic foundation

As we known, the thermodynamic flow can be considered as the function of thermodynamic force. In the equilibrium state, both of the thermodynamic force and flow of the system are equal to zero. However, for an open system that is forced to deviate from the equilibrium state, its thermodynamic forces and flows are not equal to zero any more. A thermodynamic flow can be droved by the synergy effect of one more thermodynamic force [3,4], thus this function can be defined as follows:

$$J_i = J_i(X_1, X_2, \ldots, X_{N+1}). \tag{1}$$

According to the Taylor progression, Eq. (1) can be written in detail as

$$J_i = J_{i,0} + \sum_j \left(\frac{\partial J_i}{\partial X_j}\right)_0 X_j + \frac{1}{2}\sum_j \sum_k \left(\frac{\partial^2 J_i}{\partial X_j\, \partial X_k}\right)_0 X_j X_k + \cdots. \tag{2}$$

When the system is near the equilibrium state, the effect of the thermodynamic force must be very small. The first term in the right of Eq. (2) is near to zero, and the terms after the second can be neglected. Simplifying Eq. (2), we have

$$J_i = \sum_j \left(\frac{\partial J_i}{\partial X_j}\right)_0 X_j. \tag{3}$$

Eq. (3) is the phenomenological relationship between the thermodynamic force and the thermodynamic flow. The phenomenological coefficient is defined as follows:

$$L_{ij} = \left(\frac{\partial J_i}{\partial X_j}\right)_0. \tag{4}$$

Introducing Eq. (4) into Eq. (5), we obtain

$$J_i = \sum_j L_{ij} X_j \tag{5}$$

The transfer coefficient is defined as $K_i = \left(\sum_j L_{ij} X_j\right) / X_i$, therefore $j_i = K_i X_i$ is obtained, where K_i is the non-linear function of the thermodynamic force.

According to the phenomenological theory, the rate of entropy production in irreversible process is defined as the product of thermodynamic force and thermodynamic flow [5].

$$\sigma = \sum_i J_i X_i. \tag{6}$$

For the combined system of the reaction and separation, Eq. (6) becomes

$$\sigma = J_q X_q + \sum_j^M J_j X_j + \sum_k^N J_k A_k. \tag{7}$$

where J_q is rate of heat transfer; J_j is rate of mass transfer of component I; J_k: reaction rate of reaction k and M, N are number of components and reactions, respectively.

The value of the rate of the entropy production was used to judge the direction of the process. Thermodynamic forces are expressed as follows:

$$X_q = \nabla\left(\frac{1}{T}\right) \quad \text{(temperature gradient)}. \tag{8}$$

$$X_j = -\frac{\nabla \mu_j}{T} \quad (j = 1 - M) \quad \text{(chemical potential gradient)}. \tag{9}$$

$$A_k = -\frac{1}{T}\sum_j \mu_j \nu_{jk} \quad k = 1 - N \quad \text{(chemical affinity)}. \tag{10}$$

2.2. Mass transfer rate

According to the traditional chemical engineering theory, generalized flow j is caused by the generalized force j. For example, the mass transfer is caused by the concentration gradient; the heat transfer is caused by the temperature gradient. However, according to the theory of filed synergy, the fact that force i can cause flow j should also be considered [6–9].

In the reactive distillation process coupled membrane separation, chemical potential gradient, temperature gradient, chemical reaction and membrane separation are the primary factors that affect the mass transfer rate. The effect of reaction and membrane separation appears in the mass transfer equation as the source terms. The general equation of mass transfer in this case can be written as:

$$J_i = \sum_{j=1}^M L_{ij} X_j + L_{iq} X_q + J_{im} + R_i. \tag{11}$$

Here, the first term in the right of Eq. (11) is the diffusion caused by concentration gradient; the second term is the diffusion caused by temperature gradient; the last two terms are the membrane separation and reaction, respectively. L_{ij} is defined as [10]

$$L_{ij} = -\frac{c}{R} M_i M_j D_{ij}^0 \omega_j. \tag{12}$$

where c is total mole concentration; M_i, M_j formula weight of i and j components, respectively; D_{ij}^0 diffusion coefficient of i component through j component in ideal mixed flow and ω_j

is eccentric factor of j component, which is a dimensionless quantity.

The following parameters are defined as follows:

$$D_{ij} = -\frac{c}{RT} M_i M_j D_{ij}^0 \omega_j$$

(diffusion coefficient ($mol^2\ m^{-1}\ J^{-1}\ s^{-1}$)). (13)

$$D_{iT} = \frac{L_{iq}}{T} \quad \text{(coefficient of Soret effect (mol m}^{-1}\ \text{s}^{-1}\text{))}. \tag{14}$$

The mass transfer flux J_{im} of the membrane separation consists of two parts. One is the diffusion flux J_{im}^1 caused by the chemical potential gradient; the other is infiltration flux J_{im}^2 caused by the pressure gradient. Thus, we have

$$J_{im} = J_m^1 + J_{im}^2 \tag{15}$$

where

$$J_{im}^1 = -D_{im} \nabla \mu_{im}, \tag{16}$$

$$J_{im}^2 = -P_i(\Delta p_i - \sigma \Delta \pi_{iff}). \tag{17}$$

where D_{im} is diffusion coefficient in the membrane; P_i is osmotic coefficient; σ is reflect factor and $\Delta\pi_{iff}$ is the valid osmotic pressure

The reaction rate of component i in reaction k can be defined as

$$-r_{ik} = \frac{-\nu_{ik}\dot{\xi}_k}{S_g V} \tag{18}$$

Reaction rate in terms of per specific area of catalyst becomes

$$-r'_{ik} = \frac{-r_{ik}}{S_g} \tag{19}$$

where S_g is the specific area of catalyst. Then the source term of mass transfer caused by chemical reaction can be expressed as

$$R_i = -\sum_{k=1}^{N} r_{ik} = -\sum_{k=1}^{N} \frac{\nu_{ik}\dot{\xi}_k}{S_g V}. \tag{20}$$

Introducing these terms above into Eq. (11) and rearranging, finally we obtain the rate of mass transfer J_i as following:

$$J_i = -\sum_{j=1}^{M} D_{ij} \nabla \mu_j - \frac{D_{iT}}{T} \nabla T - D_{im} \nabla \mu_{im} - P_i(\Delta p_i - \Delta \pi_{iff}) - \sum_{k=1}^{N} \frac{\nu_{ik}\dot{\xi}_k}{S_g V}. \tag{21}$$

According to $J_i = K_i \nabla \mu_i$, the coefficient of mass transfer could be expressed as

$$K_i = \frac{\sum_{j=1}^{M} D_{ij} \nabla \mu_j + \frac{D_{iT}}{T} \nabla T + D_{im} \nabla \mu_{im} + P_i(\Delta p_i - \Delta \pi_{iff}) + \sum_{k=1}^{N} \left(\frac{\nu_{ik}\dot{\xi}_k}{S_g V} \right)}{\nabla \mu_i}. \tag{22}$$

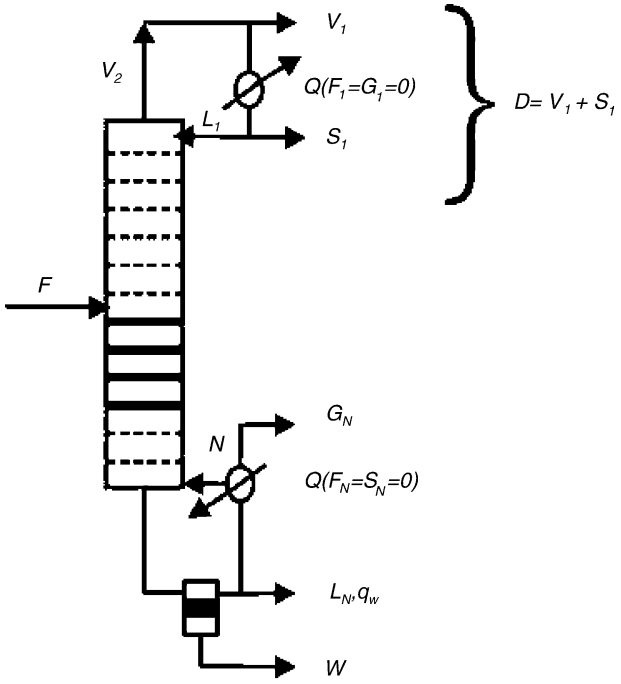

Fig. 1. Schematic diagram of the system.

Eq. (22) is a general expression of mass transfer coefficient. It shows the mass transfer rate is the function of chemical potential gradients, temperature gradients, membrane separation and chemical reaction.

For this non-ideal system, the component activity coefficients were introduced to express the chemical potential gradients as:

$$\nabla \mu_i = RT \left[\sum_{j=1}^{n-1} \left(\frac{\delta_{ij}}{x_i} + \frac{\partial \ln \gamma_i}{\partial x_j} \right) \right] \nabla x_i, \quad i, j = 1, 2, \ldots, n-1. \tag{23}$$

3. Multi fields synergy model

The non-equilibrium stage model considering multi-fields synergy for the process of reactive distillation with pervaporation which is shown as Fig. 1 is based on the following assumptions:

1. The reactions occur only in the liquid phase.
2. Both vapor and liquid phase are ideally mixed.
3. Internal mass transfer resistance of the catalyst is negligible.
4. The permeation of other components through the membrane except water is negligible.

(1) Material balance equation

Condenser : $V_2 y_{2i} - V_1 y_{1i} - (L_1 + S_1^L)x_{1i} = 0.$ (24)

Stripping and rectifying sections:

Vapor phase $V_{j+1}y_{j+1,i} - (1 + S_j^V)V_j y_{ji} + F_j^V Z_{ji}^V - N_{ji}^V = 0.$ (25)

Liquid phase $L_{j-1}x_{j-1,i} - (1 + S_j^L)L_j x_{ji} + F_j^L Z_{ji}^L + N_{ji}^L = 0.$ (26)

Reaction section:

Vapor phase $V_{j+1}y_{j+1,i} - (1 + S_j^V)V_j y_{ji} + F_j^V Z_{ji}^V - N_{ji}^V = 0.$ (27)

Liquid phase $L_{j-1}x_{j-1,i} - (1 + S_j^L)L_j x_{ji} + F_j^L Z_{ji}^L + \upsilon_i R_j + N_{ji}^L = 0.$ (28)

Reboiler : $L_{N-1}x_{N-1,i} - (1 + S_N^V)V_N y_{Ni} - L_N x_{Ni} - N_{im} = 0.$ (29)

(2) Energy balance equation

Condenser : $V_2 H_2^V - V_1 H_1^V - (L_1 + S_1^L)H_1^L - Q_1 = 0.$ (30)

Stripping and rectifying sections:

$$V_{j+1}H_{j+1}^V + L_{j-1}H_{j-1}^L - (1 + S_j^V)V_j H_j^V - (1 + S_j^V)L_j H_j^L + F_j^V H_j^{VF} + F_j^L H_j^{LF} - Q_j^V - Q_j^L = 0. \quad (31)$$

Reaction section:

$$V_{j+1}H_{j+1}^V + L_{j-1}H_{j-1}^L - (1 + S_j^V)V_j H_j^V - (1 + S_j^V)L_j H_j^L + F_j^V H_j^{VF} + F_j^L H_j^{LF} - Q_j^V - Q_j^L + (-\Delta H_r)R_j\upsilon_t = 0. \quad (32)$$

Reboiler : $(1 + S_N^V)V_N H_N^V - L_{N-1}H_{N-1}^L + L_N H_N^L + Q_N + N_m H_m = 0$ (33)

(3) Mass transfer equation

$$N_{ji}^V = N_{ji}^L = N_{ji}. \quad (34)$$

According to Eq. (21), the equation above can be written as

$$N_{ji} = J_{ji}\alpha_e. \quad (35)$$

where α_e is the effective area for the mass transfer.

(4) Phase equilibrium equation

$$y_{ji} = k_{ji}x_{ji}. \quad (36)$$

(5) Pervaporation equation

$$N_m = 0.022 x_{H_2O} A_m \,(\mathrm{mol\,s^{-1}}) \quad (37)$$

(6) Summation conditions

$$\sum_{i=1}^{C} y_{ji} = 1; \qquad \sum_{i=1}^{C} x_{ji} = 1. \quad (38)$$

The non-equilibrium stage model with synergy will yield a set of non-linear algebraic equations, which are solved by the Newton–Raphson method. This algorithm takes a three-tier approach in which the complex physical properties are approximated at the outer loop while the model equations are solved at the middle loop and inner loop. The iteration variables of inner loop, middle loop and outer loop are liquid composition at the interface, vapor and liquid bulk composition, vapor and liquid traffic, respectively. The initial guess was given from the simulation results based on the equilibrium stage model on the same operation condition. Jacobian Matrix is a diagonal matrix, which is obtained by analytical method and difference method. Fig. 2 shows the calculation flow chart in detail.

4. Kinetics and thermodynamics

The synthesis of ethyl *tert*-butyl ether (ETBE) from ethanol (EtOH) and *tert*-butyl alcohol (TBA) is accompanied by the undesired parallel dehydration of TBA using ion exchange resin. An additional side reaction is the etherification reaction of ethanol and isobutene (IB). Thus, the three considered main and side reactions are:

$$\mathrm{EtOH + TBA \Leftrightarrow ETBE + H_2O}$$

$$\mathrm{TBA \Leftrightarrow IB + H_2O}$$

$$\mathrm{EtOH + IB \Leftrightarrow ETBE}$$

Taking the inhibition of water into account, the following rate expressions are used to describe the kinetics of ETBE synthesis [11,13].

$$R_1 = Q_{cat}W_{cat}\frac{(k_{10}C_{TBA}C_{EtOH} - k'_{10}C_{ETBE}C_{H_2O})}{(1 + K_W C_{H_2O}^2)} \,(\mathrm{mol\,s^{-1}}) \quad (39)$$

$$R_2 = Q_{cat}W_{cat}\frac{(k_{20}C_{TBA} - k'_{20}C_{IB}C_{H_2O})}{(1 + K_W C_{H_2O}^2)} \,(\mathrm{mol\,s^{-1}}) \quad (40)$$

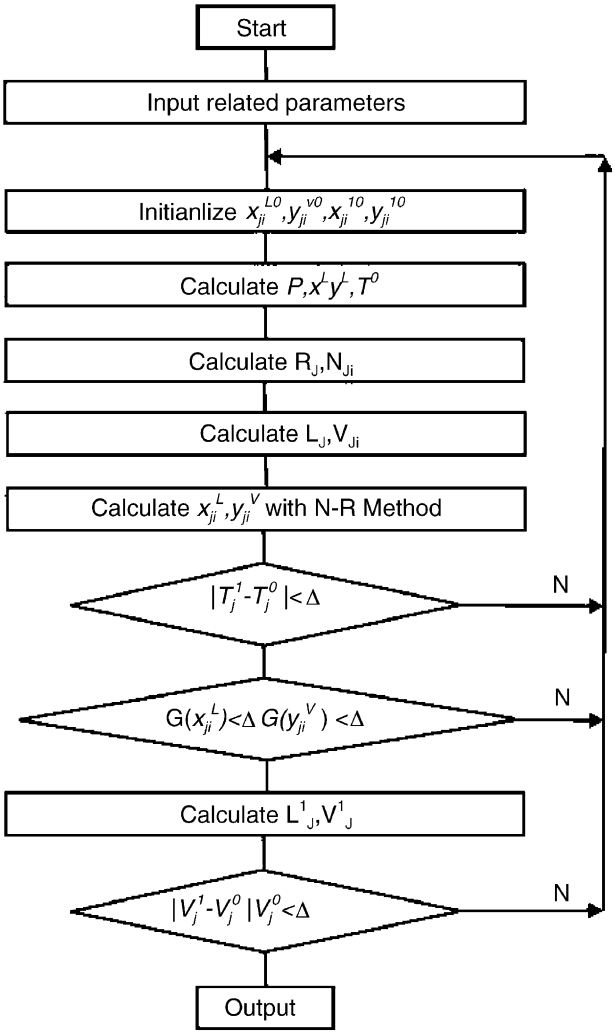

Fig. 2. Flow chart for calculation.

Table 1
Rate constants and inhibition coefficients of water

k_i Pellets	Unit
$k_{10} = \exp(-3.38-6900/T)$	$m^6\ mol^{-1}\ s^{-1}\ (mol\text{-}H^+)^{-1}$
$k'_{10} = \exp(11.19 - 11770/T)$	$m^6\ mol^{-1}\ s^{-1}\ (mol\text{-}H^+)^{-1}$
$k_{20} = \exp(15.39-10270/T)$	$m^3\ s^{-1}\ (mol\text{-}H^+)^{-1}$
$k'_{20} = \exp(1.22 - 7420/T)$	$m^6\ mol^{-1}\ s^{-1}\ (mol\text{-}H^+)^{-1}$
$k_{30} = \exp(5.71-9556/T)$	$m^6\ mol^{-1}\ s^{-1}\ (mol\text{-}H^+)^{-1}$
$k'_{30} = \exp(16.77 - 10860/T)$	$m^3\ s^{-1}\ (mol\text{-}H^+)^{-1}$
$K_W = \exp(-35.62 + 7530/T)$	$m^6\ mol^{-2}$

$$R_3 = Q_{cat} W_{cat} \frac{(k_{30} C_{IB} C_{EtOH} - k'_{30} C_{ETBE} C_{H_2O})}{(1 + K_W C^2_{H_2O})} \quad (mol\ s^{-1}) \tag{41}$$

The reaction rate constants and inhibition coefficient of water used in this work are given in Table 1.

For this strongly non-ideal system, the vapor–liquid equilibrium equation should be written as:

$$y_i \hat{\phi}_i^V P = x_i \gamma_i f_i^0 \tag{42}$$

where P is system pressure; $\hat{\phi}_i^V$ is the fugacity coefficient of gas phase, which is calculated by the virial equation. f_i^o is the fugacity of pure component at system temperature and pressure, which is given by the Poynting equation. Vapor pressure of pure component is calculated from the Antoine equation. The liquid phase activity coefficients are represented by the Wilson equation. The thermodynamic data for phase equilibrium are given in Tables 2 and 3 [12,13].

5. Experimental

A microporous hollow fibre membrane module (made by Daicel Chemical Industry Co., Japan) was used in this work. The membrane was composed of polyacrylonitrile (support layer) and a poly-ion complex (permselective layer). The membrane module system consisted of 220 hollow fibers

Table 2
Physical properties of reaction components

	EtOH	TBA	ETBE	H_2O	IB
T_c (K)	516.0	506.2	512.99	647.3	417.9
P_c (Pa)	6.383475×10^6	3.971940×10^6	3.025000×10^6	2.204832×10^7	4.002337×10^6
ω	0.635	0.618	0.3055	0.344	0.19
ANT1	-0.757609×10^2	0.2174757×10^2	0.202698937×10^2	-0.313974×10^2	20.64557002
ANT2	-0.3100647×10^4	-0.265829×10^4	−2456.489881	-0.2046366×10^4	−2125.75
ANT3	-0.4050064×10^2	-0.955×10^2	−64.91	-0.7540224×10^2	−33.15
ANT4	$-0.8814077 \times 10^{-1}$	0.0	0.0	$-0.12054280 \times 10^{-1}$	0.0
ANT5	0.2081208×10^2	0.0	0.0	0.9165751×10	0.0
ANT6	0.5045333×10^{-4}	0.0	0.0	0.489195×10^{-17}	0.0
ANT7	0.2×10	0.0	0.0	0.6×10	0.0
CPIG1	0.90141804×10	0.48612935×10^2	0.26626526×10^1	0.32242547×10^2	0.142128×10^2
CPIG2	0.21407108	0.71719884	0.64706022	0.19238346×10^2	0.281316
CPIG3	$-0.839034572 \times 10^{-4}$	$-0.70840656 \times 10^{-3}$	$-0.3963778 \times 10^{-3}$	$0.10554923 \times 10^{-4}$	-0.109494×10^{-3}
CPIG4	$0.13732704 \times 10^{-8}$	$0.29198743 \times 10^{-6}$	$0.11133251 \times 10^{-6}$	$-0.35964612 \times 10^{-8}$	0.91266×10^{-8}
$\Delta H_{V,b}$ ($J\ mol^{-1}$)	0.38769768×10^5	0.39062844×10^5	0.31751×10^5	0.40683136×10^5	0.22106052×10^5

$B = RT_c/P_c \quad [(0.083 - 0.422)/(T/T_c)^{1.6} + \omega \times \{(0.139 - 0.172)/(T/T_c)^{4.2}\}]$ ($m^3\ mol^{-1}$). $\ln(P^S) = ANT1 + ANT2/(T + ANT3) + (ANT4 \times T) + ANT5 \times \ln(T) + ANT6 \times T^{ANT7}$ (Pa), T in (K). $Cp = CPIG1 + (CPIG2 \times T) + (CPIG3 \times T^2) + (CPIG4 \times T^3)$ ($J\ (mol\ K)^{-1}$), T in (K).

Table 3
Wilson binary interaction coefficients

Component		λ_{ji} (J mol^{-1})	λ_{ji} (J mol^{-1})
i	*j*		
EtOH	TBA	3954.1	−3470.4
	ETBE	5286.5	−1034.8
	H_2O	1046.8	3975.0
	IB	5003.3	3045.4
TBA	ETBE	2366.5	230.5
	H_2O	−358.8	7944.9
	IB	5628.7	−387.4
ETBE	H_2O	12923.1	8780.1
	IB	723.1	−526.3
H_2O	IB	15819.0	22940.6

with an ID/OD of 500/800 μm and a length of 0.37 m. The pervaporation experiment results showed that the membrane module had very high water transport selectivity and it can be effective for removing water from reactant mixtures.

As the catalysts, strong cation exchange resin was formed in cylindrical pellets and fixed in the reactive distillation column. The ion exchange capacity of the resin was 3.46 mol/(kg dry pellet).

In a stander run, an equimolar mixture of EtOH and TBA was placed in the bottom and heated up to the boiling point. When the boiling point was reached, the reactant mixture was feed into the column and the operation was started up. Simultaneously, the vacuum pump was started to permeate water. Samples were taken and analyzed with a gas chromatograph.

6. Results and discussion

To predict the process behavior, the reactive distillation column was modeled using sixteen stages including a partial condenser and a partial reboiler. Stages 1 and 16 are the condenser and reboiler respectively; stages from 2 to 7 are the rectification zone; stages from 8 to 12 are the reaction section where the etherification was carried out; stages from 13 to 15 are the stripping zone. A mixture of TBA, EtOH is fed to the column on the stage 4. The basic operating parameters are shown in Table 4.

6.1. Model validation

The traditional non-equilibrium model neglects the interaction between mass, heat and chemical reaction which has an effect on the mass transfer co-efficient in reality. In this multi-fields synergy model the interaction was taken into account. The model with synergy can reflect the real process better so that the simulation results using this model should be more close to experiment results. The comparison of simulation results between the model with synergy and the model without synergy is shown in Table 5. From this table, the simulation results with synergy agree better with experiment results [2]. Thus, for the simulation of reactive distillation it is a better choice to use non-equilibrium stage modeling with synergy.

Table 4
Parameters values for the base case in the simulation

Parameters	Value
Column pressure (Pa)	101325
Distillate to feed ratio (*D*/*F*)	0.5
Ratio of vapour to distillate	0.3
Reflux ratio	5
Catalyst weight per stage (kg)	25
Feed flow rate (mol s^{-1})	1.0
Feed molar ratio (EtOH:TBA)	1:1
Feed temperature (K)	333

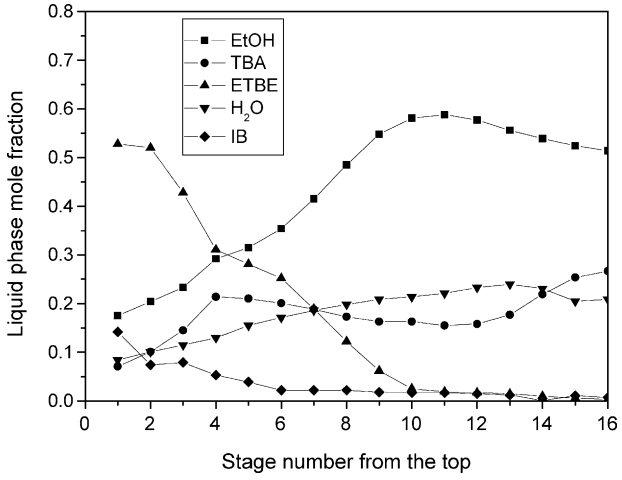

Fig. 3. Liquid phase mole fraction profile.

6.2. Column profile

Fig. 3 shows the liquid phase profiles in the column. It can be known that the concentration distributions in the column for each component show the different pattern. The fractions of TBA and H_2O in liquid phase varied slightly; however,

Table 5
Comparison of experimental and simulated product compositions

Compositions (mol%)	Condenser					Reboiler				
	EtOH	TBA	ETBE	H_2O	IB	EtOH	TBA	ETBE	H_2O	IB
Experimental data	15.6	7.9	53.5	7.7	15.3	50.0	27.0	0.0	23.0	0.0
Simulation data (with synergy)	17.5	7.1	52.8	8.4	14.2	51.4	26.7	0.3	20.9	0.7
Simulation data (without synergy)	20.5	1.8	52.3	9.7	15.6	56.5	36.5	0.01	7.0	0.0

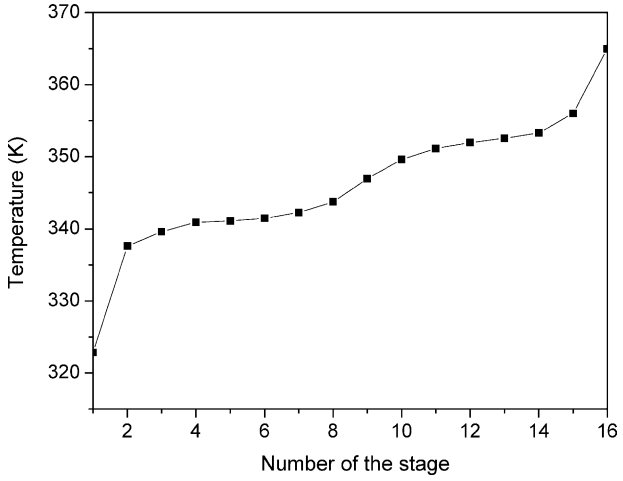

Fig. 4. Temperature profile.

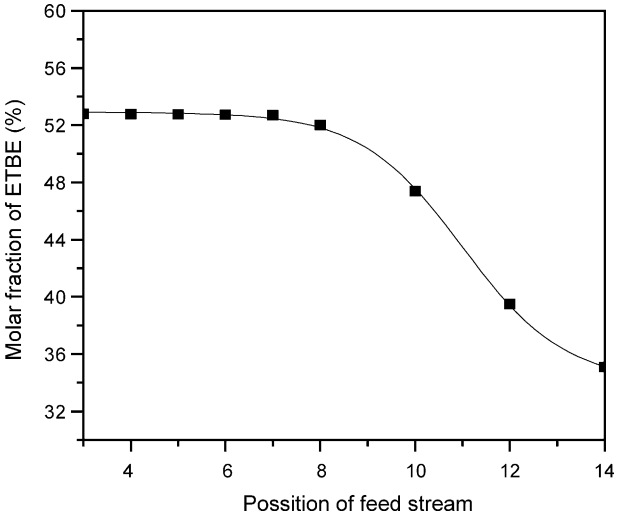

Fig. 6. Effect of feed position on ETBE purity.

the fraction of ETBE becomes richer quickly above stage 10. From the top to the bottom, the mole fraction of EtOH increases first, and then decreases slowly. IB is easily volatized and is rising to the top. These variations are mainly due to the differences of the volatility for each component.

The temperature profile shows that the temperature decreases monotonously from the bottom to the top of the column in Fig. 4. The temperatures in the reaction zone are flat and most of the reaction occurs in narrow range.

6.3. Effect of reflux ratio

The effect of the reflux ratio is shown in Fig. 5. It can be known that the increasing the reflux ratio from 0 to 3 significantly increases the concentration of ETBE in the distillate. This is a result of increased separation efficiency, which in turn shifts the reaction to produce ETBE. However, this tendency becomes weak when reflux ratio increases continuously. The reason can be considered the inhibition effect of water to the catalyst and the azeotropic properties. A high reflux ratio is economically unattractive as it adds to the equipment size and energy requirements.

6.4. Effect of feed position

The effect of feed position to the concentration of ETBE in the distillate is shown in Fig. 6. When the feed position is above the eighth stage, the purity of ETBE does not change obviously; however, the purity of ETBE decreases quickly when feed position is changed from stages 8 to 14.

6.5. Effect of molar feed ratio of EtOH to TBA

The feed composition significantly affects the concentration of ETBE in the distillate as shown in Fig. 7. As the

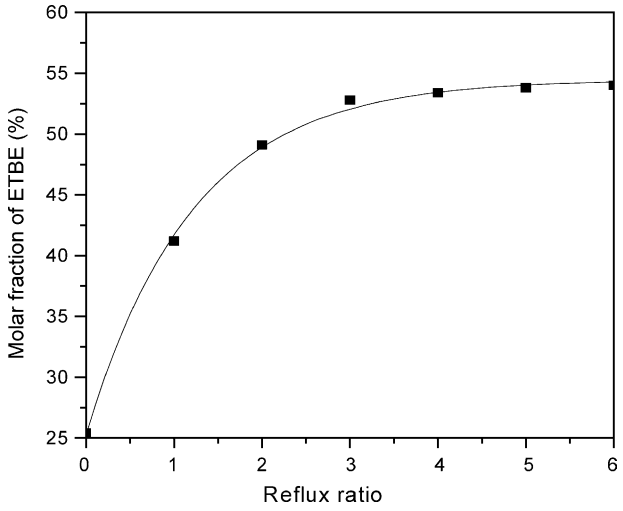

Fig. 5. Effect of reflux ratio on the ETBE purity.

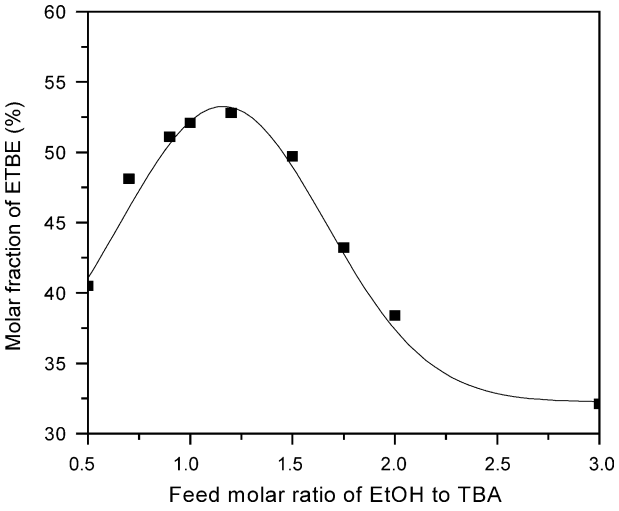

Fig. 7. Effect of feed composition on ETBE purity.

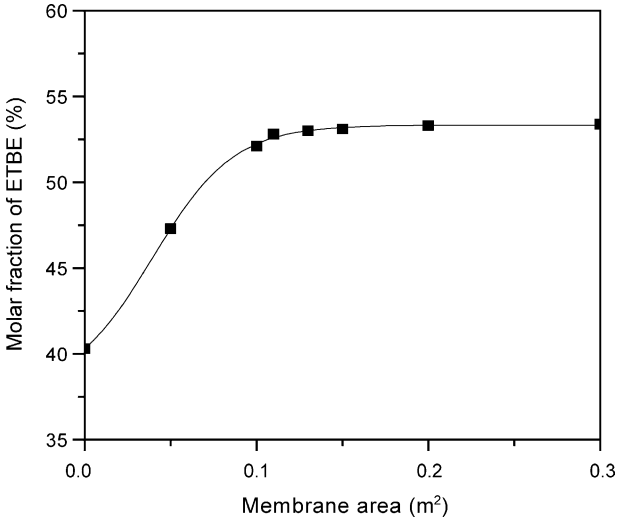

Fig. 8. Effect of membrane area on ETBE purity.

increasing of the ratio of EtOH/TBA, the purity of the ETBE goes up first, then, it goes down quickly. The reason can be considered as following: since the dehydration of TBA into IB and water could be inhibited by increasing the ratio of EtOH/TBA, the selectivity of ETBE can also be increased. However, higher ratio of EtOH/TBA will increase the separation duty or decrease the product purification for the reason that the ETBE-EtOH azeotropic mixture is formed easily. The suitable feed ratio of EtOH/TBA will be 1.2 as shown in Fig. 5.

6.6. Effect of membrane area

Fig. 8 shows the effect of membrane area on the concentration of ETBE in the distillate. The bigger the membrane area is, the more water produced is removed from the system. Therefore, higher purity of ETBE will be obtained. However, when the membrane area increases up to 0.15 m^2, the concentration of ETBE becomes constant. The reason can be considered as following: when the membrane area increase further, the reaction rate becomes the main controlling step, since the catalyst loading is constant, thus a larger membrane area offers no benefits to improvement of conversion and ETBE purity.

7. Conclusion

Synergy of fields in the process of reactive distillation coupled membrane separation by using phenomenological theory is analyzed. From the viewpoint of multi-field synergy, a new model was developed to analyze the process of reactive distillation coupled with membrane separation. Simulation results with the theory of multi-fields synergy agree well with the experimental results.

Acknowledgements

Financial support for this work from the Key Project of National Natural Science Foundation of China (20436040) and the National Natural Science Foundation of China (20176044) is gratefully acknowledged.

Appendix A. Nomenclature

A	chemical affinity (J mol^{-1} K)
A_m	membrane area (m^2)
c	component mole concentration (mol m^{-3})
D	coefficient of diffusion (m^2 s^{-1})
F	feed flow rate, mol s^{-1})
h	molar enthalpy of vapor mixture (J mol^{-1})
H	molar enthalpy of liquid mixture (J mol^{-1})
H_m	pervaporation enthalpy of water (J mol^{-1})
J	thermodynamic flow
K	coefficient of transfer
L	phenomenological coefficient
M	molecular weight
N	mass transfer rate (mol s^{-1})
P	pressure (Pa)
R	rate of reaction (mol s^{-1})
Q	heat duty
T	temperature (K)
x	liquid mole fraction
y	vapor mole fraction

Greek symbols

δ_{ij}	Kronecker delta ($\delta_{ijj} = 1$ for $i = j$, $\delta_{ijj} = 0$ for $i \neq j$)
γ_i	activity coefficient of component i (dimensionless)
λ	coefficient of heat conduction (J m^{-1} K^{-1} s^{-1})
μ	chemical potential (J mol^{-1})
π	pressure of infiltration (Pa)
σ	rate of entropy production
ω	acentric factor
ξ	extent of reaction (mole)

References

[1] B.L. Yang, S. Goto, Pervaporation with distillation for the production of ethyl *tert*-butyl ether, Sep. Sci. Tech. 32 (1997) 971–981.
[2] S.B. Yang, B.L. Yang, Catalytic reactive distillation coupled with pervaporation for synthesizing ethyl *tert*-butyl ether, J. Chem. Ind. Eng. 52 (2001) 950–956.
[3] G. Han, B. Hua, Q. Chen, et al., The general energy expression and energy state postulate, J. South China Univ. Tech. (Chinese version) 29 (2001) 48–50.
[4] R. Li, Non-equilibrium Thermodynamics and Dissipative Structure, Tsinghua University Press, Beijing, 1986.
[5] G. Nicolis, I. Prigogine, Self-organization in Non-equilibrium Systems, Science Press, Beijing, 1986.
[6] X.H. Tao, B.L. Yang, B. Hua, Analysis for fields synergy in the reactive distillation process, J. Chem. Eng. Chin. Univ. 17 (2003) 389–394 (in Chinese).

[7] M. Shi, M. Yao, The cross effect of thermal and water vapor transfer for textiles, J. Northwest Inst. Sci. Tech. (Chinese version) 15 (2001) 29–32.
[8] M.S. Malashetty, S.N. Gaikwad, Effect of cross diffusion on double diffusive convection in the presence of horizontal gradients, Inter. Eng. Sci. 40 (2002) 773–787.
[9] G. Gong, C. Mei, P. Zhou, Discussion on some concepts of coupling problem of multi-field in numerical simulation, J. Hunan Univ. (Chinese version) 26 (1999) 71–77.
[10] J.C. Slattery, Momentum Energy and Mass Transfer in Continua, McGraw Hill Inc., New York, 1978.
[11] B.L. Yang, S.B. Yang, R.Q. Yao, Synthesis of ethyl *tert*-butyl ether from *tert*-butyl alcohol and ethanol on strong acid cation-exchange resins, React. Funct. Polym. 44 (2000) 167–175.
[12] B.L. Yang, H.J. Wang, Vapor liquid equilibrium for mixtures of water, alcohols and ethers, J. Chem. Eng. Data 47 (2002) 1324–1329.
[13] B.L. Yang, S.B. Yang, H.J. Wang, Simulation for the reative distillation process to synthesize ethyl *tert*-butyl ether, J. Chem. Eng. Japan 34 (2001) 1165–1170.